

Protective effects of an anti-melanocortin-4 receptor scFv derivative in lipopolysaccharide-induced cachexia in rats

Jean-Christophe Peter · Hélène Rossez ·
Marjorie Weckering · Géraldine Zipfel ·
Anne-Catherine Lecourt · Joshua B. Owen ·
William A. Banks · Karl G. Hofbauer

Received: 1 June 2012 / Accepted: 2 August 2012
© Springer-Verlag 2012

Abstract

Background Cachexia is a complex syndrome defined by weight loss due to an ongoing loss of skeletal muscle mass with or without loss of body fat. It is often associated with anorexia. Numerous results from experimental studies suggest that blockade of the melanocortin-4 receptor (MC4R) could be an effective treatment for anorexia and cachexia. In a previous study, we reported the basic pharmacological properties of a blocking anti-MC4R mAb 1E8a and its scFv derivative in vitro and in vivo.

Methods In the present study, we further characterized the mode of action of the 1E8a scFv, evaluated its pharmacokinetic properties in mice, and assessed its therapeutic potential in a lipopolysaccharide (LPS)-induced cachexia model in rats.

Results In vitro, scFv enhanced the efficacy of the endogenous inverse agonist Agouti-related protein. After intravenous (i.v.) administration in mice, the scFv penetrated the blood–brain barrier (BBB) and reached its central sites of action: the scFv brain–serum concentration ratios increased

up to 15-fold which suggests an active uptake into brain tissue. In telemetry experiments, i.v. administration of the scFv in rats was well tolerated and only induced slight cardiovascular effects consistent with MC4R blockade, i.e., a small decrease in mean arterial pressure and heart rate. In the model of LPS-induced anorexia, i.v. administration of scFv 1E8a prevented anorexia and loss of body weight. Moreover, it stimulated a myogenic response which may contribute to the preservation of muscle mass in cachexia.

Conclusion The pharmacological profile of scFv 1E8a suggests its potential value in the treatment of cachexia or anorexia.

Keywords Monoclonal antibody · scFv derivative · Melanocortin-4 receptor · Cachexia · Anorexia · Lipopolysaccharide

1 Introduction

Cachexia is a complex syndrome associated with diverse underlying diseases such as malignant tumors, infection and inflammation, cardiac insufficiency, renal or hepatic failure, and chronic obstructive pulmonary disease [1, 2]. Considerable efforts are devoted to a better definition of this syndrome and its different stages. According to a recent consensus paper, cachexia is defined by weight loss resulting from an ongoing loss of skeletal muscle mass with or without loss of body fat [3]. These processes are the consequence of a negative protein and energy balance often associated with signs of inflammation. Loss of appetite (anorexia) is another pathogenic factor which contributes to the development of a negative energy balance in these

J.-C. Peter · H. Rossez · M. Weckering · G. Zipfel ·
A.-C. Lecourt · K. G. Hofbauer
Applied Pharmacology, Biozentrum, University of Basel,
Basel, Switzerland

J.-C. Peter · K. G. Hofbauer (✉)
Obexia AG, c/o Biozentrum,
50/70 Klingelbergstrasse,
CH-4056 Basel, Switzerland
e-mail: karl.hofbauer@unibas.ch

J. B. Owen · W. A. Banks
VAPSCHS, GRECC/S-182 and Division of Gerontology
and Geriatric Medicine, Department of Internal Medicine,
University of Washington School of Medicine,
Seattle, WA, USA

patients. Many of these changes are caused by the increased production of cytokines which are generated by cells of the immune system but also in the brain microvasculature and microglia [4].

The negative impact of cachexia on morbidity and mortality has only been recognized in recent years. Consequently, increasing research activities are being spent on the elucidation of the basic mechanisms underlying the pathophysiology of cachexia [3, 5]. Although remarkable progress in preclinical and clinical research has been achieved in recent years, the currently available treatment options are still limited. The cachectic state cannot be overcome by nutritional support alone, and only a couple of largely ineffective drugs are available for pharmacotherapy. The most widely used of these drugs is megestrol acetate, a gestagen with glucocorticoid effects. However, under megestrol treatment, patients mainly accumulate body fat which raises their body weight but does not improve muscular strength and physical performance [1].

Numerous data from experimental studies suggest that blockade of the melanocortin-4 receptor (MC4R) could be an effective treatment for anorexia and cachexia [4, 6–9]. In previous studies, we have shown that immunization against the N-terminal sequence of the MC4R leads to the generation of polyclonal antibodies (Abs) that block the receptor by acting as inverse agonists and non-competitive antagonists [10, 11]. Our subsequent efforts to produce monoclonal Abs (mAbs) resulted in a molecule with a unique mechanism of action [12]. The mAb 1E8a acts (1) as an inverse agonist suppressing the basal constitutive activity of the receptor, (2) as a non-competitive antagonist inhibiting the effects of the endogenous agonist α -melanocortin-stimulating hormone, and (3) as a potentiator of the endogenous inverse agonist Agouti-related protein (AgRP).

In a previous study, we reported the basic pharmacological properties of the mAb 1E8a and its scFv derivative in vitro and in vivo. In the present study, we further characterized the mode of action of the scFv, evaluated its pharmacokinetic properties, and assessed its therapeutic potential in a lipopolysaccharide (LPS)-induced cachexia model. Due to unique properties, the scFv penetrates the blood–brain barrier (BBB) and reaches its central sites of action also after intravenous (i.v.) administration, while the complete mAb has to be given intracerebroventricularly. Moreover, after i.v. administration of the scFv brain–serum concentration, ratios of up to 15-fold were reached, which suggest an active uptake into brain tissue. These favorable pharmacodynamic and pharmacokinetic properties make the scFv 1E8a a promising candidate for further development for the treatment of anorexia and cachexia [12].

2 Material and methods

2.1 Animals

Male Sprague Dawley rats, 6 weeks old at the beginning of the experiments (initial body weight approximately 200 g), were used for all pharmacodynamic studies. Rats were obtained from Charles River (Charles River Laboratories, L'Arbresle, France) and kept at a 12-h light/dark cycle (lights on from 6:00 a.m. to 6:00 p.m.) in a room with constant temperature (22 °C) and humidity (50 %). Rats were housed individually 1 week before the beginning of an experiment and were given free access to tap water and standard laboratory chow (NAFAG 3432, 3.0 kcal/g, 61.6 % of total calories from carbohydrate, 24.8 % from protein, and 13.6 % from fat; Nafag Ecosan, Gossau, Switzerland).

Male CD-1 mice were used for the pharmacokinetic studies. They were anesthetized with urethane. All animal studies were conducted in accordance with international standards and protocols approved by the local animal use committee.

2.2 Telemetry transmitter implantation

Rats were anesthetized by inhalation of isoflurane (4 % for induction and 2 % for maintenance). The operation area was shaved, disinfected with iodine, and a 4–5-cm midline abdominal incision was made. The intestines were gently retracted with saline-soaked sterile gauze permitting access to the abdominal aorta from the renal arteries to the iliac bifurcation. The abdominal aorta was separated from the vena cava distal to the renal arteries. To occlude temporarily the abdominal aorta, a vascular clamp (Fine Science Tools GmbH, Heidelberg, Germany) was used. While the abdominal aorta was clamped, the catheter of the telemetry transmitter (TL11M2-C50-PXT, Data Sciences International, Warwick, RI, USA) was inserted and secured with a single drop of tissue adhesive (Vetbond™, 3 M, St. Paul, MN, USA). The vascular clamp was removed, and the catheter entry site was checked for leakage. The transmitter was sutured to the inside surface of the peritoneum, and the abdominal and skin incisions were closed with a non-absorbable suture (Ethicon®, silk 3-0 and Prolene® 4-0, respectively [Ethicon, Somerville, NJ, USA]). All procedures were performed aseptically and according to the recommendations of the manufacturer (Data Sciences International, USA).

2.3 Radiotelemetric monitoring

Values for body temperature (BT), mean arterial pressure (MAP), heart rate (HR), and locomotor activity (Act) were recorded via telemetry as described previously [13]. An

evaluation time of 20 s every 30 min was selected. The monitoring was performed over a period of 24 h to establish for each rat its own baseline week 0. The animals were then recorded for 24 h once a week. The telemetric data were analyzed as the difference between mean values obtained over a period of 24 h before and during LPS injection.

2.4 LPS injection

At the end of the study (week 20), a single intraperitoneal injection of 75 $\mu\text{g}/\text{kg}$ lipopolysaccharide from E-coli (Sigma, Switzerland) was performed at 5:00 p.m. Body weight and food intake were monitored for 5 days.

2.5 Blood and tissue harvesting

Fasted rats were killed by decapitation under isoflurane anesthesia. One milliliter of blood was collected in ice-cooled EDTA-treated tubes and the rest, in ice-cooled untreated tubes after decapitation. Blood was centrifuged at $4600 \times g$ for 20 min at 4 °C, and the plasma and serum were kept at -20 °C.

2.6 cAMP assays

HEK-293 cells expressing the human MC4R (hMC4R) were distributed in 24-well plates. On the day of stimulation, cells were washed with DMEM (Sigma) for 4 h at 37 °C and incubated in DMEM supplemented with 100 μM 3-isobutyl-1-methyl-xanthine (IBMX) (Sigma) for 1 h at 37 °C. For the treatment in presence of α -MSH, dilutions were performed in PBS, 0.1 % BSA and 100 μM IBMX. Dilutions of α -MSH (Bachem AG, Bubendorf, Switzerland) from 0.1 to 10 μM were added (15 min) with or without pre-treatment with 1E8a scFv (30 min). Cells were lysed with Biotrak cAMP lysis buffer, and cAMP content was measured using the Biotrak cAMP enzyme immunoassay system (GE Healthcare Bio-Sciences, Uppsala, Sweden) according to manufacturer's instructions. Protein concentration of the samples was determined using a BCA Kit. The ratio between the concentration of cAMP and protein was calculated in order to normalize results as a function of cell number/wells. This ratio was expressed as percentage of maximum cAMP content.

2.7 Expression of scFv

Rosetta bacteria transformed with pET22b(+)-1E8a or pET22b(+)-2 G2 grown in 500 ml of medium 2xYT (bactotryptone 1.6 %, bacto yeast extract 1 %, NaCl 0.5 %, pH 7.0) containing ampicilline of 0.15 mM (Applichem, Darmstadt, Germany) and chloramphenicol of 0.1 mM (Gerbu Biotechnik, Gaiberg, Germany) until an $\text{OD}_{600 \text{ nm}}$ of 0.6, (37 °C with

agitation at 200 rpm). The expression of scFv was induced by adding 1 mM IPTG (Applichem, Darmstadt, Germany) at room temperature for 4 h.

2.8 Periplasmic extraction

Five hundred milliliters of bacteria cultures were centrifuged (10 min, 10,000 g, 4 °C), and the pellet was resuspended in 200 ml of TES (Tris 30 mM, EDTA 1 mM, sucrose 2 %, pH 8.5). After centrifugation (10 min, 10,000 g, 4 °C), the pellet was resuspended in 50 ml MgSO_4 5 mM. After a last centrifugation (10 min, 10,000 g, 4 °C), the supernatant corresponding to the periplasmic extract (PE) was collected. This PE was dialyzed in wash buffer NiNTA (imidazole 20 mM, Na_2HPO_4 50 mM, NaCl 300 mM, pH 8.0) overnight at 4 °C.

2.9 Purification of scFv

The scFv were purified from the PE on NiNTA columns according to the manufacturer's instruction (Qiagen). After elution, purified scFv was dialysed in PBS (NaCl 276 mM, Na_2HPO_4 20.3 mM, KCl 5.4 mM, KH_2PO_4 3.5 mM) overnight at 4 °C. The scFs was then purified by immunoadsorption as described previously in [12]. The concentrations were determined with Micro BCA Protein Assay kit (Pierce, Rockford, IL, USA).

2.10 Control mAb and scFv

Control mAb and scFv (2 G2) were described in [12] as pharmacologically inactive on the MC4R.

2.11 Intracerebroventricular and intravenous administration

Male Sprague Dawley rats (275–325 g) were anesthetized with isoflurane in medicinal oxygen (4 % for induction and 2 % for maintenance of anesthesia). A stainless steel cannula (26 gauge, 10-mm long) was implanted into the third cerebral ventricle using the following coordinates, relative to the Bregma: -2.3 mm anteroposterior, 0 mm lateral to the midline, and -7.5 mm ventral to the surface of the skull. The guide cannula was secured in place with three stainless steel screws and glass-ionomer cement (3 M), and a stylet was inserted to seal the cannula until use. Temgesic (Essex Chemie AG, Lucerne, Switzerland) (0.03 mg/kg) was given subcutaneously prior to and for 2 days post surgery. Seven days after recovery from surgery, accuracy of the cannula placement in the third ventricle was tested by measuring the dipsogenic response (immediate drinking of at least 5 ml water in 15 min) to an intracerebroventricular (i.c.v.) injection of 20 pmol of angiotensin II in 2- μl injection volume.

The purified mAb was slowly (1 min) injected i.c.v. at 9:00 a.m. at a dose of 1 µg in a volume of 3 µl by using a Hamilton syringe. These doses were selected based on the results of comparative in vitro studies. Following the injection of mAb, food intake was continuously recorded during the following 3 days using an automatic food intake apparatus (TSE Systems, Bad Homburg, Germany) at 1 h intervals.

In the experiments with i.v. administration, purified scFv 1E8a and BSA were injected into the tail vein of rats at 9:00 a.m. and 5:00 p.m. under mild isoflurane anesthesia at a dose of 100, 300, and 1,000 µg/kg prior to LPS administration at the beginning of the dark phase (6:00 p.m.). Following the injection of LPS, food intake was continuously recorded using an automatic food intake apparatus (TSE Systems) at 1-h intervals for 2 days.

2.12 RNA extraction and real-time quantitative PCR

Frozen tissues were homogenized under liquid nitrogen, and total RNA was isolated using Trizol reagent (Invitrogen). RNA concentrations were adjusted, and reverse transcription was carried out using random hexamer primers (Promega). Real-time PCR analysis (Power SYBR Green Master Mix, Applied Biosystems) was performed using the ABI Prism 7000 Sequence Detector. Relative expression levels for each gene of interest were calculated with the $\Delta\Delta C_t$ method and normalized to the expression of the glyceraldehyde 3-phosphate dehydrogenase (GAPDH). Primers used for the amplification of the gene of interest are listed in Table 1.

2.13 Radioactive labeling and purification

The scFv 1E8a protein was radioactively labeled with ^{125}I by the Chloramine-T method. Five micrograms of scFv

Table 1 Oligonucleotide primers used in real-time RT-PCR

Product	Primers name	Sequence (5'-3')
IGF-1	IGF-1 for	GCTATGGCTCCAGCATTCG
	IGF-1 rev	TCCGGAAGCAACTCATCC
Myogenin	Myogenin for	TGCCACAAGCCAGACTACCCACC
	Myogenin rev	CGGGGCACTCACTGTCTCTCA A
MyoD	MyoD for	GGAGACATCCTCAAGCGATGC
	MyoD rev	AGCACCTGGTAAATCGGATTG
MRF4	MRF4 for	AGAGACTGCCCAAGGTGGAGATTC
	MRF4 rev	AAGACTGCTGGAGGCTGAGGCATC
GAPDH	GAPDH for	TGCACCACCAACTGCTTA
	GAPDH rev	GGATGCAGGGATGATGTTCC

IGF-1 insulin-like growth factor-1, *MRF4* myogenic regulatory factor 4, *GAPDH* glyceraldehyde 3-phosphate dehydrogenase

solubilized in phosphate buffer solution (pH 7.4) was incubated with 2 µCi of ^{125}I and chloramine-T reagent (10 µl of 1 mg/ml) for 60 s. The chloramine-T reaction was stopped with the addition to the reaction mixture of sodium metabisulfite (10 µl of 10 mg/ml). The resultant ^{125}I -scFv was purified from any unincorporated ^{125}I by the use of G-10 Sephadex column. The first five fractions represented void volume with radioactive material appearing in subsequent fractions. The resultant fractions were counted, and the fractions with the highest count per minute (CPM) values were selected for acid precipitation assays. Five micrograms of bovine serum albumin (BSA) was iodinated with 2 µCi of ^{131}I and processed according to the same procedure described above for scFv.

2.14 Acid precipitation

To determine the purity of scFv iodination fractions from the G-10 Sephadex purification step, 5 µl of the highest CPM fractions was added to 500 µl of 1 % BSA. Five hundred microliters of 30 % trichloroacetic acid was added to mixture and allowed to stand for 3 min. The solution was centrifuged at 5,000×g for 10 min, and the supernatant was decanted from the resultant pellet. The pellet and supernatant were counted and used in the following formula to determine the percentage of iodination:

$$\% \text{Iodination} = \frac{\text{CPM pellet}}{\text{CPM pellet} + \text{CPM supernatant}} \times 100.$$

2.15 Pharmacokinetics of brain influx

The blood-to-brain unidirectional influx constant (K_i ; in units of microliters per gram per minute) was calculated using multiple-time regression analysis [14, 15]. Briefly, the right jugular vein and left carotid artery were exposed. At $t=0$, 0.2 ml of lactated Ringer's solution containing 1 % BSA (LR-BSA) and 500,000 cpm ^{125}I -scFv were injected into the jugular vein. Between 2 and 180 min after the intravenous injection, blood was collected from the carotid artery, and the mouse was immediately decapitated. The brain was removed and weighed. Two mice were used for each time point. The arterial blood was centrifuged, and serum was collected, and results were graphed and expressed as the brain/serum ratio (in units of microliters per gram) and plotted against exposure time (Expt):

$$\text{Expt} = \left[\int_0^t \text{Cp}(\tau) d\tau \right] / \text{Cpt},$$

where Cp is the level of radioactivity in serum, and Cpt is the level of radioactivity in serum at time t . Expt values correct for the clearance of the test substance from the blood

so that the greater the clearance from blood, the greater the difference between Expt and *t*. Without Expt corrections, the K_i would be overestimated. Brain/serum ratios were calculated by dividing the CPM values obtained from each brain by the individual brain weight. The slope of the linear portion of the relation between brain/serum ratios and Expt measures K_i (microliters per gram per minute) and the intercept of the linearity measures V_i (microliters per gram), the initial volume of distribution in the brain.

To test for the presence of a saturable influx system, male CD-1 mice were anesthetized with urethane and given doses of ^{125}I -scFv in increasing doses of 0.1, 1.0, and 10 $\mu\text{g}/\mu\text{l}$ unlabeled scFv and sacrificed 1 h post injection. Blood and brain were collected and counted as described above.

2.16 Pharmacokinetics of brain efflux

Brain-to-blood transport of scFv was determined by methods previously described [16]. In brief, 25,000 CPM of ^{125}I -scFv was injected into the lateral ventricle of urethane anesthetized CD-1 male mice via an i.c.v. injection and decapitated at time points of 0, 2, 5, 10, 20, and 30 min post injection ($n=6$ per time point). Mice used for time point 0 were sacrificed with an overdose of urethane, given an i.c.v. injection, and immediately decapitated. The above experimental conditions were used for an experiment where CD-1 mice were injected with 25,000 CPM scFv + 0.54 $\mu\text{g}/\mu\text{l}$ unlabeled scFv. Brains were counted, and the resultant CPM values were transformed into the percentage of injection remaining in the brain via the following formula:

$$\% \text{ Injection remaining in brain} = \frac{\text{Brain CPM}}{\text{Average injection check CPM}} \times 100.$$

Three injection checks were performed during the experiment where 1 μl of injectate was added to a glass vial and counted with the brains post experiment. The average of the injection check values was used in the formula above. Values of Log % injection remaining in the brain were plotted against time.

2.17 Data analysis

All data are expressed as mean \pm SD or SEM as indicated. Data were analyzed by two-way ANOVA repeated measures with Bonferroni post hoc test or by Student *t* test using Graph pad Prism 4 software. For the cAMP concentration-response experiments, the best fitting curves were compared for their minimum, maximum, and EC_{50} using *F* test. K_i and EC_{50} were calculated using Graph pad Prism 4 software.

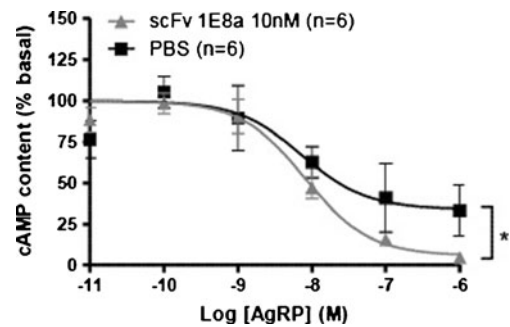


Fig. 1 Intracellular cAMP production in HEK-293 cells transfected with hMC4R. **a** Concentration–response curves obtained with AgRP in the presence of 10 nM of scFv 1E8a (triangle) or PBS (black square). The increased efficacy of AgRP in the presence of scFv 1E8a suggests that it acts in synergy with AgRP. Data are presented as means \pm SD as calculated from three independent experiments

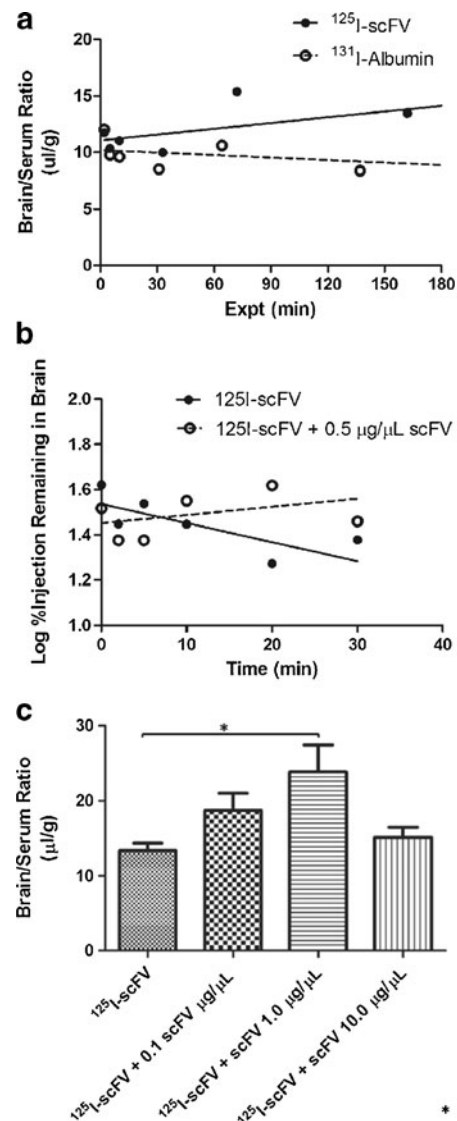


Fig. 2 **a** Comparison of I-scFv and I-albumin uptake by whole brain. **b** Competition of I-scFv with scFv uptake by whole brain. **c** Comparison of I-scFv and I-scFv+scFv uptake by whole brain

3 Results

3.1 Pharmacological properties of scFv 1E8a in vitro

HEK-293 cells overexpressing hMC4R were treated with increasing concentrations of AgRP in the presence or absence of scFv 1E8a (10 nM). Intracellular cAMP accumulation was measured upon treatment. The presence of scFv 1E8a induced a higher efficacy of AgRP, i.e., a stronger inverse agonistic effect (Fig. 1).

3.2 Pharmacokinetic properties of scFv 1E8a in mice

Figure 2a shows the uptake of ^{125}I -scFv and ^{131}I -albumin into whole brain after i.v. injection. A significant correlation between brain/serum ratio and exposure time (Expt) was observed for scFv ($r=0.606$, $n=13$, $p<0.05$), showing that scFv is transported across the BBB with an influx constant, K_i , of 0.0171 ± 0.0071 $\mu\text{l/gmin}$. No significant correlation between brain/serum ratio and exposure time (Expt) was observed for ^{131}I -albumin, indicating that the BBB was intact in the experimental model system, and the transfer of scFv was not the result of BBB damage. Figure 2c shows that increasing dosages of scFv increased the rate of scFv transfer into the brain across the BBB. Such a paradoxical increase is a hallmark of saturable efflux systems. At the highest dose used (10 μg scFv/ μl), transport was shown to be decreased compared to lower doses, suggesting that there may also be an influx system on the luminal side of the BBB for scFv. An i.c.v. study was conducted to test this hypothesis of the existence of an efflux system, and Fig. 2b shows that efflux from the brain to the blood across the BBB occurred with a half-time clearance of 35.7 min ($K_i=-0.008435\pm 0.003690$, $r=0.391$, $n=36$, $p<0.05$). The

addition of non-radiolabeled scFv (0.5 $\mu\text{g}/\mu\text{l}$) decreased efflux, suggesting the presence of an efflux system. Statistical comparison of these two lines showed a significant reduction of slope with the addition of unlabeled scFv ($p<0.05$). Further studies were conducted utilizing scFv doses ranging from 0.05 to 0.15 μg scFv/ μl of non-radiolabeled material also inhibited transport. These studies indicate that saturable efflux and probably influx transport systems determine the degree to which scFv crosses the BBB.

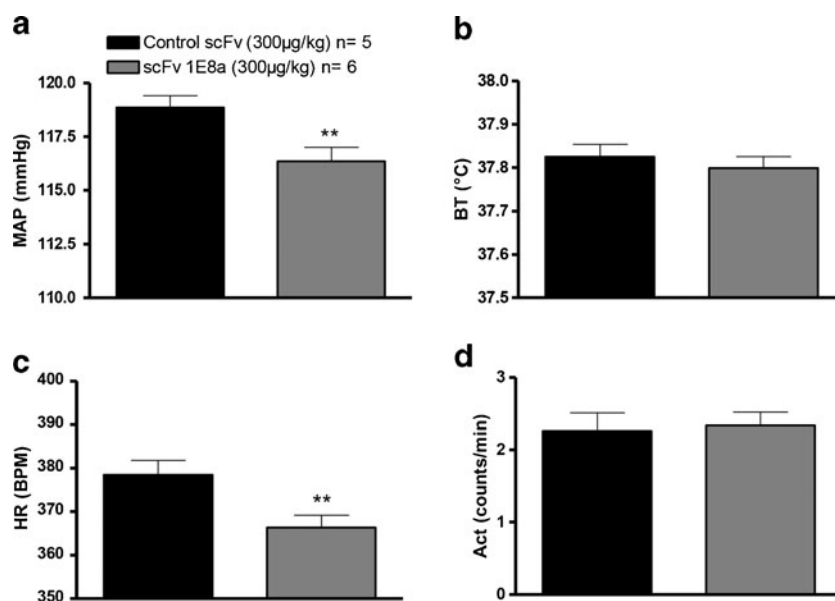
3.3 Safety pharmacology of scFv 1E8a in conscious rats

Rats received an i.v. injection of scFv 1E8a or a control scFv at 9:00 a.m., i.e., during the light phase. MAP, BT, HR, and Act were continuously recorded during the following 24 h. Rats which received scFv 1E8a showed a significant decrease in MAP and HR as compared with controls (Fig. 3a, c). Neither BT nor Act was affected by the treatment (Fig. 3b, d).

3.4 Effect of an i.c.v. injection of mAb 1E8a on LPS-induced anorexia in rats

mAb 1E8a or a control mAb was administrated i.c.v. in the third ventricle of rats 1 h prior to LPS administration (75 $\mu\text{g}/\text{kg}$ i.p.) at the beginning of the light phase (6:00 p.m.). LPS injection at this concentration induced a 50 % reduction in food intake and a significant decrease in body weight over the first 48 h. Rats which received mAb 1E8a showed a significant gradual increase in food intake (Fig. 4a). The loss in body weight was less pronounced over the first 24 h, and a faster recovery was observed over the second 24 h as compared with controls (Fig. 4b).

Fig. 3 Change in **a** mean arterial pressure, **b** body temperature, **c** heart rate, or **d** locomotor activity over 24 h following i.v. administration of scFv 1E8a or control scFv. Rat which received scFv 1E8a showed a significant decrease in MAP and HR as compared with controls (*double asterisks* $p<0.01$, Student's *t* test). Neither BT nor Act was different between the two groups during this period



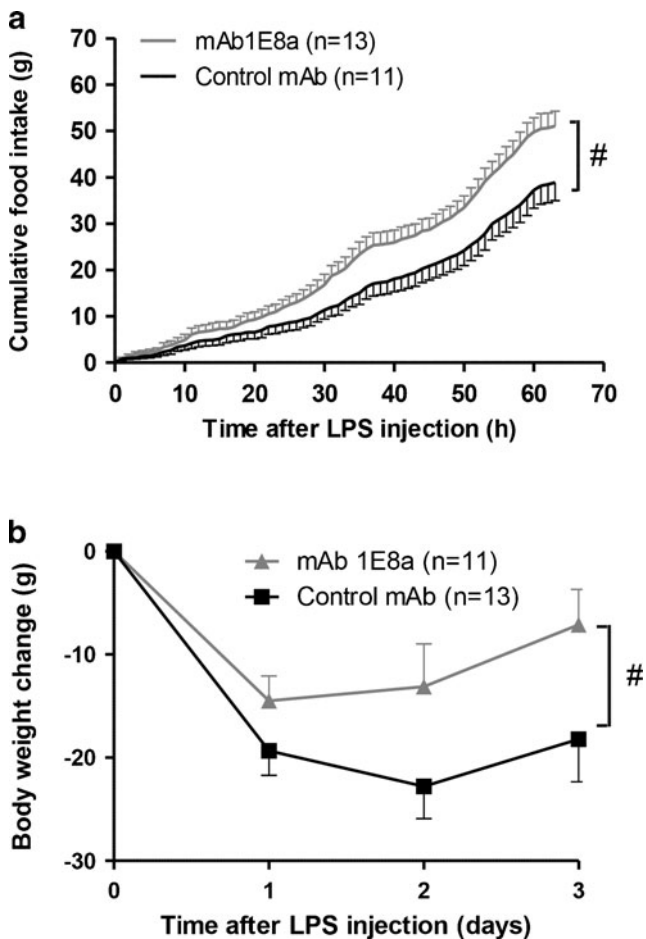


Fig. 4 **a** Sixty-two-hour food intake of rats that received an i.c.v. injection of 1 μ g of mAb 1E8a or 1 μ g of control mAb 30 min prior to an i.p. injection of LPS (75 μ g/kg). Rats which received mAb 1E8a gradually and significantly increased their food intake as compared with control rats ($p < 0.05$, two-way ANOVA with repeated measures). **b** Evolution of body weight in rats that received an i.c.v. injection of 1 μ g of mAb 1E8a or 1 μ g of control mAb 30 min prior to an i.p. injection of LPS (75 μ g/kg). Rats which received mAb 1E8a gradually and significantly increased their body weight as compared with control rats ($p < 0.05$, two-way ANOVA with repeated measures)

3.5 Effect of an i.v. injection of scFv 1E8a on LPS-induced anorexia and the expression of myogenic factors in rats

Rats received scFv 1E8a at concentrations of 100, 300, or 1,000 μ g/kg by i.v. administration. Rats were treated twice (9.00 a.m. and 5:00 p.m.) prior to LPS administration at the beginning of the dark phase (6:00 p.m.). Figure 5 shows cumulative food intake and body weight change after LPS administration. Rats which received scFv 1E8a showed a dose-dependent significant increase in food intake and body weight as compared with control rats (Fig. 5).

When the expression of IGF-1, Myogenin, MyoD, and Myogenic regulatory factor 4 in the gastrocnemius muscle of rats was measured using real-time RT-PCR, it was found to be consistently increased in a dose-dependent manner (Fig. 6).

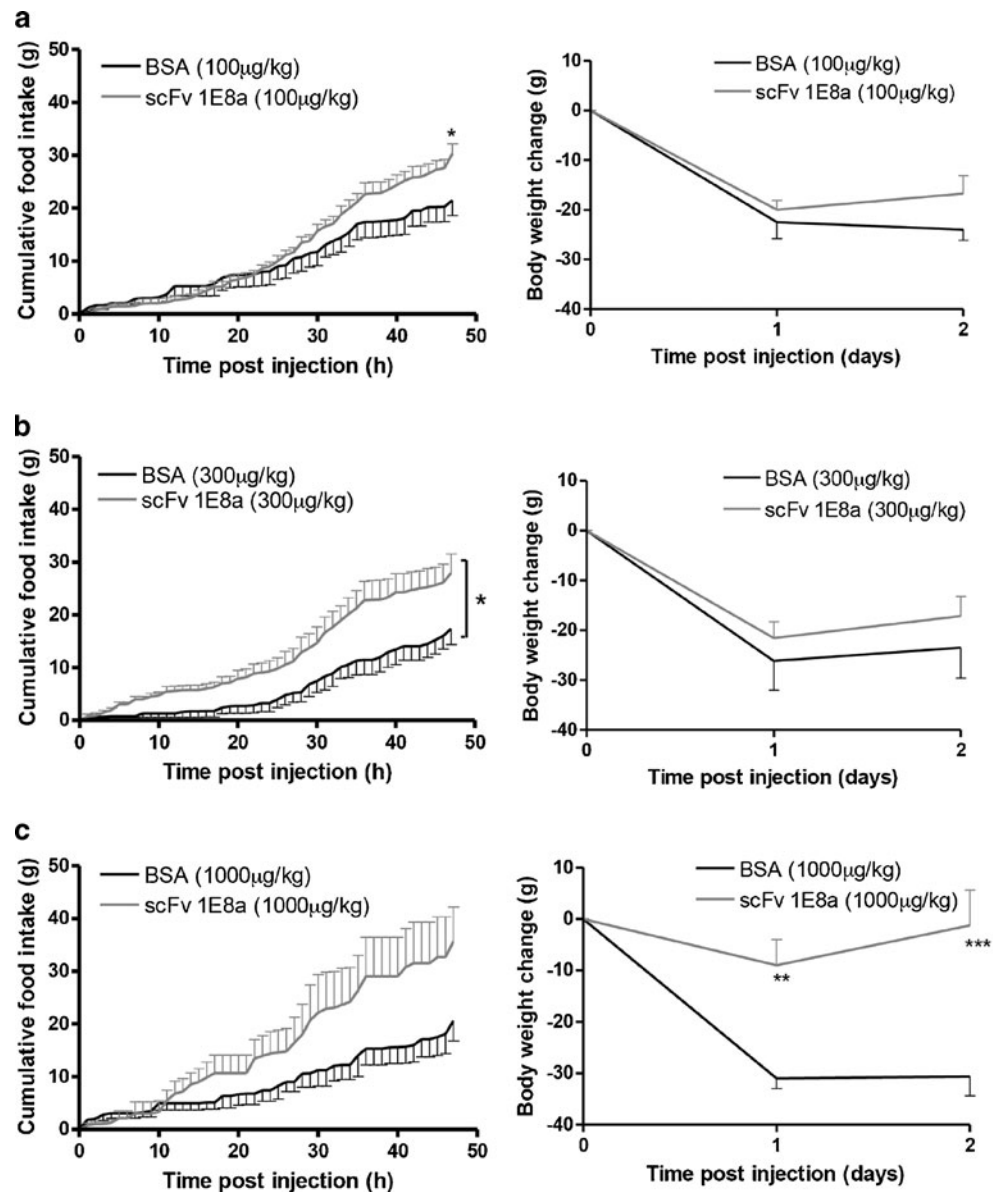
4 Discussion

In previous studies, we have shown that mAb 1E8a and its scFv derivative acted as inverse agonists and non-competitive antagonists of the MC4R. We also observed that mAb 1E8a acted synergistically with the endogenous inverse agonist AgRP and shifted its concentration-response curve to the left [12]. In the present study, we observed that the scFv also enhanced the inverse agonist effect of AgRP but increased its maximum efficacy. The difference between the effects of the complete mAb and its scFv derivative may be explained by the fact that the mAb exerted a more pronounced steric hindrance leading to a higher affinity as compared with the scFv.

Pharmacokinetic studies were conducted in mice to characterize the extent of scFv brain penetration. scFv brain influx rates were significantly higher than the influx rates of the vascular marker albumin. This is indicative of a transport of scFv across the BBB via mechanisms that are independent of extracellular pathways and pathways associated with IgG and IgM proteins [17–19]. An experiment using increased amounts of non-radiolabeled scFv was conducted to characterize the transport mechanism of scFv across the BBB. The results of this experiment showed a statistically significant increase in influx at the low concentration of non-radiolabeled scFv (1.0 μ g/ μ l), but not at the high concentration (10.0 μ g/ μ l). A potential reason for this increase in the brain/serum ratio is that an efflux system is present on the abluminal side of the BBB. This paradoxical transport behavior has been previously shown to occur with an antagonist against growth hormone-releasing hormone [20]. The unlabeled scFv was not at a sufficient concentration to inhibit influx but did inhibit the efflux system. An i.c.v. study demonstrated that co-injection with non-radiolabeled scFv inhibited efflux at all doses tested (0.05–0.5 μ g per mouse). These results are consistent with saturable influx and efflux systems for scFv.

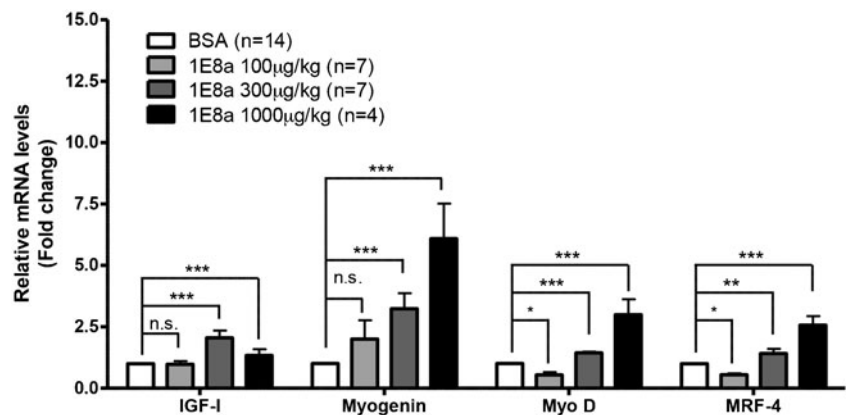
Passage of antibodies from blood-to-brain is largely restricted by the blood–brain barrier (BBB). However, there is a residual leakiness of the BBB at a number of sites referred to in general as the extracellular pathways [21]. We have shown that antibodies are able to use this pathway to access the brain in concentrations that can affect the CNS [18, 22, 23]. Some antibodies, such as IgG's [24, 25], are also transported in the brain-to-blood direction by a saturable process, whereas other antibodies, such as IgM's, are not [23]. Our results here and in a previously published paper show that the scFv fragment of the antibody crosses the BBB much better than albumin and IgG molecules [12]. This indicates that scFv uses some pathway in addition to the extracellular pathways to access the brain. One likely mechanism for scFv passage is that of adsorptive transcytosis, a broad category used by a variety of substances that

Fig 5 Cumulative food intake (left panels) and body weight changes (right panels) of rats that received, 8 and 1 h prior to an LPS i.p. injection (75 $\mu\text{g}/\text{kg}$), three different doses of scFv 1E8a of 100 $\mu\text{g}/\text{kg}$ (*n*=7) (a); 300 $\mu\text{g}/\text{kg}$ (*n*=7) (b); and 1,000 $\mu\text{g}/\text{kg}$ (*n*=4) (c) or BSA as control at 100 $\mu\text{g}/\text{kg}$ (*n*=6) (a); 300 $\mu\text{g}/\text{kg}$ (*n*=7) (b); and 1,000 $\mu\text{g}/\text{kg}$ (*n*=3) (c). Rats which received scFv 1E8a increased their food intake and body weight as compared with controls in a dose-dependent manner (*n.s.* non-significant; single asterisk $p<0.05$, double asterisks $p<0.01$, triple asterisks $p<0.001$, Student's *t* test)



depends on interactions between glycoproteins on the brain endothelial cell and charged regions of the transported molecule [26–28].

Fig. 6 Myogenic factor gene expression in rats that received, 8 and 1 h prior to an LPS i.p. injection (75 $\mu\text{g}/\text{kg}$), three different doses of scFv 1E8a or BSA as control: 100, 300, and 1,000 $\mu\text{g}/\text{kg}$. Rats that received scFv 1E8a increased significantly muscle genesis biomarkers in a dose-dependent manner as compared with control rats (*n.s.* non-significant; single asterisk $p<0.05$, double asterisks $p<0.01$, triple asterisks $p<0.001$, Student's *t* test)



The safety and tolerability of an i.v. administration of the scFv derivative was demonstrated in conscious rats chronically instrumented for telemetry studies. After a dose of 300

$\mu\text{g}/\text{kg}$, rats showed a significant decrease in MAP and HR. No decrease in Act or BT was observed, indicating that behavioral changes are not responsible for this effect. Stimulation of the MC4R has been described to increase sympathetic tone [29]. It is therefore likely that MC4R blockade lead to a decrease of MAP and HR via a reduction in sympathetic activity.

In further *in vivo* experiments, we tested the protective effect of the complete mAb and its scFv [12] in LPS-induced anorexia [30–33]. It has been shown that in this model, an inflammatory response to cytokines leads to an activation of the POMC axis and the stimulation of the MC4R results in acute anorexia [34].

The mAb 1E8a was given *i.c.v.*, while the scFv was given *i.v.* In either case, MC4R blockade lead to a significant increase in food intake and prevented the loss of body weight in this disease model. The effects of the scFv showed a clear dose-dependency. With increasing doses, the duration of the effects was also prolonged. Moreover, it was observed that myogenic factors were increased in a dose-dependent manner in rats which received scFv 1E8a. These effects were significant within 24 h of administration which suggest that they may be directly mediated by MC4R blockade and therefore depend on the establishment of an improved energy balance.

Taken together, our previous and present studies showed that the anti-MC4R scFv 1E8a has a unique mechanism of action: it is an inverse agonist, a non-competitive antagonist of the endogenous agonist α -MSH [12] and a potentiator of the endogenous inverse agonist AgRP. After *i.v.* administration, the scFv 1E8a passed the BBB and showed a brain/serum ratio of approximately 15-fold. In telemetry experiments, the scFv was well tolerated and only induced cardiovascular effects consistent with MC4R blockade. In the model of LPS-induced anorexia, peripheral administration of scFv 1E8a attenuated anorexia and loss of body weight. Moreover, it stimulated a myogenic response which may contribute to the preservation of muscle mass in this disease model. This unique pharmacological profile suggests a potential value of scFv 1E8a in the treatment of cachexia or anorexia.

Acknowledgments These studies were supported by a grant of the Swiss Anorexia Nervosa Foundation. The authors of this manuscript certify that they comply with the ethical guidelines for authorship and publishing in the *Journal of Cachexia, Sarcopenia and Muscle* [35].

Conflict of interest KGH and JCP are co-founders of Obexia AG, a start-up company devoted to the development of scFv 1E8a.

References

- Evans WJ, Morley JE, Argiles J, Bales C, Baracos V, Guttridge D, et al. Cachexia: a new definition. *Clin Nutr.* 2008;27:793–9.
- Laviano A, Inui A, Marks DL, Meguid MM, Pichard C, Rossi Fanelli F, et al. Neural control of the anorexia-cachexia syndrome. *Am J Physiol Endocrinol Metab.* 2008;295:E1000–8.
- Fearon K, Strasser F, Anker SD, Bosaeus I, Bruera E, Fainsinger RL, et al. Definition and classification of cancer cachexia: an international consensus. *Lancet Oncol.* 2011. doi:10.1016/S1470-2045(10)70218-7.
- Marks DL, Cone RD. Central melanocortins and the regulation of weight during acute and chronic disease. *Recent Prog Horm Res.* 2001;56:359–75.
- Blum D, Omlin A, Baracos VE, Solheim TS, Tan BH, Stone P, et al. Cancer cachexia: a systematic literature review of items and domains associated with involuntary weight loss in cancer. *Crit Rev Oncol Hematol.* 2011. doi:10.1016/j.critrevonc.2010.10.004.
- Marks DL, Cone RD. The role of the melanocortin-3 receptor in cachexia. *Ann N Y Acad Sci.* 2003;994:258–66.
- Marks DL, Ling N, Cone RD. Role of the central melanocortin system in cachexia. *Cancer Res.* 2001;61:1432–8.
- Nicholson JR, Kohler G, Schaerer F, Senn C, Weyermann P, Hofbauer KG. Peripheral administration of a melanocortin 4-receptor inverse agonist prevents loss of lean body mass in tumor-bearing mice. *J Pharmacol Exp Ther.* 2006;317:771–7.
- Wisse BE, Frayo RS, Schwartz MW, Cummings DE. Reversal of cancer anorexia by blockade of central melanocortin receptors in rats. *Endocrinology.* 2001;142:3292–301.
- Hofbauer KG, Lecourt AC, Peter JC. Antibodies as pharmacologic tools for studies on the regulation of energy balance. *Nutrition.* 2008;24:791–7.
- Peter JC, Nicholson JR, Heydet D, Lecourt AC, Hoebcke J, Hofbauer KG. Antibodies against the melanocortin-4 receptor act as inverse agonists *in vitro* and *in vivo*. *Am J Physiol Regul Integr Comp Physiol.* 2007;292:R2151–8.
- Peter JC, Lecourt AC, Weckering M, Zipfel G, Niehoff ML, Banks WA, et al. A pharmacologically active monoclonal antibody against the human melanocortin-4 receptor: effectiveness after peripheral and central administration. *J Pharmacol Exp Ther.* 2010;333:478–90.
- Kramer K, Kinter LB. Evaluation and applications of radiotelemetry in small laboratory animals. *Physiol Genomics.* 2003;13:197–205.
- Blasberg RG, Fenstermacher JD, Patlak CS. Transport of alpha-aminoisobutyric acid across brain capillary and cellular membranes. *J Cereb Blood Flow Metab.* 1983;3:8–32.
- Patlak CS, Blasberg RG, Fenstermacher JD. Graphical evaluation of blood-to-brain transfer constants from multiple-time uptake data. *J Cereb Blood Flow Metab.* 1983;3:1–7.
- Banks WA, Kastin AJ. Quantifying carrier-mediated transport of peptides from the brain to the blood. *Methods Enzymol.* 1989;168:652–60.
- Banks WA, Farr SA, Morley JE, Wolf KM, Geylis V, Steinitz M. Anti-amyloid beta protein antibody passage across the blood–brain barrier in the SAMP8 mouse model of Alzheimer's disease: an age-related selective uptake with reversal of learning impairment. *Exp Neurol.* 2007;206:248–56.
- Banks WA, Terrell B, Farr SA, Robinson SM, Nonaka N, Morley JE. Passage of amyloid beta protein antibody across the blood–brain barrier in a mouse model of Alzheimer's disease. *Peptides.* 2002;23(12):2223–6.
- Broadwell RD, Sofroniew MV. Serum proteins bypass the blood–brain fluid barriers for extracellular entry to the central nervous system. *Exp Neurol.* 1993;120:245–63.
- Jaeger LB, Banks WA, Varga JL, Schally AV. Antagonists of growth hormone-releasing hormone cross the blood–brain barrier: a potential applicability to treatment of brain tumors. *Proc Natl Acad Sci U S A.* 2005;102:12495–500.

21. Broadwell RD, Sofroniew MV. Serum proteins bypass the blood–brain barrier for extracellular entry to the central nervous system. *Exp Neurol*. 1993;120:245–63.
22. Banks WA, Pagliari P, Nakaoka R, Morley JE. Effects of a behaviorally active antibody on the brain uptake and clearance of amyloid beta proteins. *Peptides*. 2005;26:287–94.
23. Banks WA, Farr SA, Morley JE, Wolf KM, Geylis V, Steinitz M. Anti-amyloid beta protein antibody passage across the blood–brain barrier in the SAMP8 mouse model of Alzheimer's disease: an age-related selective uptake with reversal of learning impairment. *Exp Neurol*. 2007;206:248–56.
24. Garg A, Balthasar JP. Investigation of the influence of FcRn on the distribution of IgG to the brain. *AAPS J*. 2009;11:553–7.
25. Schlachetzki F, Zhu C, Pardridge WM. Expression of the neonatal Fc receptor (FcRn) at the blood–brain barrier. *J Neurochem*. 2002;81:203–6.
26. Banks WA, Akerstrom V, Kastin AJ. Adsorptive endocytosis mediates the passage of HIV-1 across the blood–brain barrier: evidence for a post-internalization coreceptor. *J Cell Sci*. 1998;111:533–40.
27. Raub TJ, Audus KL. Adsorptive endocytosis and membrane recycling by cultured primary bovine brain microvessel endothelial cell monolayers. *J Cell Sci*. 1990;97:127–38.
28. Terasaki T, Takakuwa S, Saheki A, Moritani S, Shimura T, Tabata S, et al. Adsorptive-mediated endocytosis of an adrenocorticotropic hormone (ACTH) analogue, ebitatide, into the blood–brain barrier: studies with monolayers of primary cultured bovine brain capillary endothelial cells. *Pharm Res*. 1992;9:529–34.
29. Ni XP, Butler AA, Cone RD, Humphreys MH. Central receptors mediating the cardiovascular actions of melanocyte stimulating hormones. *J Hypertens*. 2006;24:2239–46.
30. Gautron L, Lafon P, Tramu G, Laye S. In vivo activation of the interleukin-6 receptor/gp130 signaling pathway in pituitary corticotropes of lipopolysaccharide-treated rats. *Neuroendocrinology*. 2003;77:32–43.
31. MacDonald L, Radler M, Paolini AG, Kent S. Calorie restriction attenuates LPS-induced sickness behavior and shifts hypothalamic signaling pathways to an anti-inflammatory bias. *Am J Physiol Regul Integr Comp Physiol*. 2011;301:R172–84.
32. Marks DL, Butler AA, Turner R, Brookhart G, Cone RD. Differential role of melanocortin receptor subtypes in cachexia. *Endocrinology*. 2003;144:1513–23.
33. Sergeev V, Broberger C, Hokfelt T. Effect of LPS administration on the expression of POMC, NPY, galanin, CART and MCH mRNAs in the rat hypothalamus. *Brain Res Mol Brain Res*. 2001;90:93–100.
34. Ueta Y, Hashimoto H, Onuma E, Takuwa Y, Ogata E. Hypothalamic neuropeptides and appetite response in anorexia-cachexia animal. *Endocr J*. 2007;54:831–8.
35. von Haehling S, Morley JE, Coats AJ, Anker SD. Ethical guidelines for authorship and publishing in the *Journal of Cachexia, Sarcopenia and Muscle*. *J Cachexia Sarcopenia Muscle*. 2010;1:7–8.